An Evaluation of Tocotrienol Ethosomes for Transdermal Delivery using Strat-M® membrane and excised Human skin.

Rajesh Sreedharan Nair [a,b], Nashiru Billa [a,c], Chee-Onn Leong [d] and Andrew P. Morris [a,e]

[a] School of Pharmacy, The University of Nottingham Malaysia, Jalan Broga, 43500 Semenyih, Selangor Darul Ehsan, Malaysia.

[b] School of Pharmacy, Monash University Malaysia, Jalan Lagoon Selatan, 47500 Bandar Sunway, Selangor Darul Ehsan, Malaysia

[c] College of Pharmacy, Qatar University, QU Health, P.O. Box: 2713 – Doha, Qatar.

[d] Center for Cancer and Stem Cell Research, International Medical University, No.126, Jalan Jalil Perkasa 19, Bukit Jalil, 57000 Kuala Lumpur, Malaysia.

[e] Swansea University Medical School, Swansea University, Singleton Park, Swansea, UK.

Running head: transdermal delivery of tocotrienol ethosomes

*****Corresponding author: Rajesh Sreedharan Nair
E mail : rajeshsreedharan.nair@monash.edu
Phone No: +60355146159
Fax : +60355146364

Abstract

Tocotrienol (TRF) ethosomes were developed and evaluated *in vitro* for potential transdermal delivery against melanoma. The optimised TRF ethosomal size ranged between 64.9 ± 2.2 nm to 79.6 ±3.9 nm and zeta potential (ZP) between -53.3 mV to -62.0 ± 2.6 mV. Characterisation of the ethosomes by ATR-FTIR indicated the successful formation of TRF-ethosomes. Scanning electron microscopy (SEM) images demonstrated the spherical shape of ethosomes, and the entrapment efficiencies of all the formulations were above 66%. *In vitro* permeation studies using full-thickness human skin showed that the permeation of gamma-T3 from the TRF ethosomal formulations was significantly higher (P<0.05) than from the control. The cumulative amount of gamma-T3 permeated from TRF ethosome after 48 hours was 1.03 ± 0.24 µg cm^{-2} with a flux of 0.03 ± 0.01 µg cm^{-2} h^{-1}. Furthermore, the flux of gamma-T3 across the Strat-M® and the epidermal membrane was significantly higher than that across full-thickness human skin (p < 0.05). *In vitro* cytotoxicity studies on HaCat cells showed significantly higher cell viability than the pure drug solution (p < 0.05). The enhanced skin permeation and high cell viability associated with this formulation suggest a promising carrier for the transdermal delivery.

Keywords: transdermal, TRF, ethosomes, human skin, permeation, cell-viability.

Introduction

Palm oil is extracted from the fruit of the oil palm plant (*Elaies guineensis* and *Elaeis oleifera*). The use of fats and oils as food supplements and in cosmetics and medicines is widespread and palm oil is one of the predominant members of the fats and oils family. More than 90% of palm oil produced is used in the food industry (Mba et al. 2015). Palm oil derivatives are also heavily used, and these include palm olein, palm stearin, purified fatty acids, and fatty acid derivatives. Palm olein and palm stearin are used as bases in the formulation and manufacture of semisolid pharmaceutical dosage forms. Whereas the fatty acids present in palm oil have been shown to elicit permeation enhancement in transdermal drug delivery (TDD) and have been employed in transdermal therapeutic systems (skin patches) (Barry 2001). Palm tocotrienol-rich fractions (TRF) has a long history of safe use as a natural vitamin E source and as an antioxidant in the food industry and is certified by the US FDA as generally recognised as safe (GRAS). TRF contains >80% tocotrienols with gamma-T3 being the predominant isomer. Studies report a nano-emulsified tocotrienol formulation for dermal photoprotection and were found skin-compatible indicating its potential for topical and transdermal use (Brownlow et al. 2015; Hasan et al. 2018). The *stratum corneum* (SC) layer which can significantly control the permeation of relatively high molecular weight compounds and is considered the major limiting factor for the transdermal delivery of many drugs. Therefore, to enhance transdermal delivery, it may be necessary to employ various enhancement techniques such as chemical or physical methods or by using nanocarrier systems. Nanocarrier systems such as nanoparticles or nanovesicles possess advantages over the other methods as they promote transdermal permeation without affecting the skin's structure (Williams and Barry 2004; Manickam et al. 2019). Although nanoparticles have shown some success in transdermal delivery, the tough SC layer is still a challenging barrier (Nair Rajesh Sreedharan et al. 2019). Rapid attainment of therapeutic blood levels with a sufficient flux to maintain those concentrations remains out of

reach for many drugs. Lipid vesicles such as liposomes have shown some success in topical and transdermal delivery (Jose et al. 2018), however, liposomes are effective primarily for topical delivery with evidence of their skin permeation being limited. Given that liposomes rarely permeate much deeper than the SC, ethosomes are being evaluated as delivery systems for improving the permeation of both hydrophilic and hydrophobic drugs (Nainwal et al. 2019). A majority of studies with tocotrienols have been aimed at improving bioavailability following oral administration (Alqahtani et al. 2013, 2014). Permeation studies of TRF nanoformulations utilising human skin or similar models such as Strat-M® membrane have received much less research attention. Because of its hydrophobicity (Log *P* = 8.9) and relatively high molecular weight (410.6 g/mol) the passive diffusion of gamma-T3 through skin is extremely difficult. Studies have shown that gamma-T3 from TRF nanoemulsions can permeate across a cellulose-ester membrane (CM) (Pham et al. 2016). However, the flux values may not be directly comparable to those obtained using Strat-M® membranes (Haq et al. 2018) or human skin. CM is employed in many permeation studies but they are simple porous membranes with no inherent rate controlling property. Our research group previously reported that a TRF vehicle possessed promising skin permeation enhancing effects for the moderately lipophilic drug ibuprofen (Singh et al. 2018). TRF has been shown to possess anticancer activities against many types of cancers including melanoma (Aggarwal et al. 2003; Ling et al. 2012), and their poor aqueous solubility hinder their passage across the skin. Reports suggest that ethosomes can reach deeper skin layers due to their enhanced permeability, and this property would be beneficial in melanoma treatment (Yu et al. 2015). Hence, it was considered worth developing a suitable TRF containing ethosomes aimed at melanoma treatment and evaluate *in vitro* before commencing any biological evaluations. The main objective of this work was to assess the *in vitro* permeation profiles of TRF-ethosome formulations using specific models such as

synthetic Strat-M® membrane and excised full-thickness human skin that can provide insight into the behaviour of formulation *in vivo.*

Materials and Methods

Materials

TRF and the gamma-T3 standard were obtained from ExcelVite Sdn Bhd, Perak, Malaysia. Phosphatidylcholine from Soy Lecithin was purchased from MP Biomedicals, USA Cholesterol was purchased from Sigma Aldrich, USA. Ethanol, phosphate buffered saline (PBS-pH 7.4 Tablets) and methanol (HPLC grade) were purchased from Fisher Scientific, UK. The Strat-M® membrane and the MTT [3-(4,5-dimethylthiazol-2-yl)-2,5-diphenyltetrazolium bromide] reagent were purchased from Millipore, Merck Germany. Dulbecco's modified Eagle's medium (DMEM), polysorbate 80, penicillin-streptomycin (1%) and foetal bovine serum were purchased from Nacalai Tesque, Japan. The HaCat cells were obtained from the Center for Cancer and Stem Cell Research, International Medical University, Kuala Lumpur, Malaysia.

Methods

Formulation of tocotrienol containing ethosomes.

Ethosomes were synthesised using the thin film evaporation method with some modifications (Zhai et al. 2015). The composition of ethosomal formulations is given in Table 1. The vesicle size and the zeta potential (ZP) of ethosomes were optimised by modulating the phospholipid content, alcohol composition and sonication parameters. Firstly, Soya phosphatidylcholine (SPC)), cholesterol and polysorbate 80 were dissolved in chloroform and methanol (2:1 v/v) in a 25 mL round-bottom flask. To this mixture, TRF (10mg) was added and the binary solvent mixture allowed to evaporate using a rotary evaporator (Büchi Rotavapor® R-200, Switzerland) at 40 ˚C and 50 rpm for 30 minutes. A thin film was formed on the walls of the flask, which was redispersed in PBS containing 30 - 50% ethanol at 40 ˚C whilst rotating at 50 rpm for a

further hour and the final volume was adjusted to 10 mL. The vesicles obtained were transferred into a 50 mL centrifuge tube, kept in an ice bath (Watson, Japan) and sonicated using a probe ultrasonicator (Q Sonica, Newtown, USA) at 20% amplitude for 1 min with a pulse of 2 sec ON and 5 sec OFF sequence.

Determination of vesicle size, polydispersity index (PDI) and ZP

The average diameter, PDI and the ZP of ethosome formulations were determined using the Zetasizer Nano ZS® (Malvern Instruments, Malvern, UK) after appropriate dilution using deionised water (1:3), n=3. Although Zetasizer® is commonly used for size analysis, it does not provide details on the morphological characteristics of particles.

Scanning Transmission Electron Microscopy (STEM)

Surface morphology was studied by using a Field Emission Scanning Electron Microscope (Quanta 400F, FEI, USA) at a voltage of 5 kV and a magnification of 20,000 x. Ethosomal dispersion were placed on a copper grid using a micropipette and allowed to dry overnight at 25°C. The STEM images were recorded for the drug-loaded ethosomes and the blank preparations.

Determination of the Encapsulation efficiency (EE%)

The EE was determined by ultracentrifugation methods based on that of Heeremans et al. with some modification (Heeremans et al. 1995). The drug-loaded ethosomes kept overnight at refrigerator were ultracentrifuged (Beckman Coulter, Allegra® 64R Centrifuge) at 25,000 rpm at 4 °C for 45 minutes. The supernatant was removed and the gamma-T3 present in the supernatant, i.e. the unentrapped drug, was determined by injecting 30 µL of the sample into the HPLC system (Agilent 1290 series). A reverse phase column (Hypersil Gold C18, 250 mm length × 4.6 mm diameter), maintained at 30 °C was used for the analysis. An isocratic elution was employed with a mobile phase composition of 95:05 (methanol: water) at a flow rate of 1.1 ml/min, and the detection wavelength set at 295 nm. The total amount of drug in the

formulation was determined by lysing the ethosomes with Triton X (10%) and the resultant mixture was filtered through a 0.45 µm nylon syringe filter prior to HPLC analysis (n=3). The encapsulation efficiency was determined using equation 1:

$$EE\% = \frac{T - U}{T} \times 100 \quad \text{..... equation 1}$$

T- Total amount of gamma-T3 in the formulation

U- Unentrapped gamma-T3

Attenuated Total Reflectance – Fourier Transform Infrared Spectroscopy (ATR-FTIR)

The FTIR spectra were recorded for cholesterol, SPC, blank ethosomes, TRF, and the drug-loaded ethosome using a Perkin-Elmer ATR-FTIR spectrophotometer (Perkin Elmer, USA). The crystal surface was cleaned using acetone to remove contaminants, which would have caused interference on the spectrum. A background scan was run first and then a pinch of sample was placed on the diamond crystal surface and scanned from 4000-400 cm^{-1} over 36 scans having a resolution of 4 cm^{-1} at an interval of 1 cm^{-1}.

***In vitro* permeation experiments**

Permeant solubility studies in the receptor phase

The saturation solubility of TRF was determined in PBS pH 7.4, PBS pH 7.4 containing 1% polysorbate 80 and PBS pH 7.4 with 40% ethanol. The solubility of the permeant in these vehicles was determined by adding an excess quantity to the vehicle and shaking in a thermoregulated incubator shaker at 37 °C and 200 rpm for 72 hours. The samples (n=3) were then filtered using a 0.45 µm nylon syringe filter and the drug content was analysed using the HPLC methods outlined in earlier sections.

***In vitro* permeation studies of TRF-ethosomes using Strat-M® membrane**

The *in vitro* permeation of the selected ethosomal formulations was evaluated across Strat-M® membrane by using static Franz-type diffusion cells according to our previously reported

method (Nair Rajesh Sreedharan et al. 2019). The donor and the receptor compartments of the diffusion cells were having capacities of 1 mL and 2 mL respectively with an effective permeation area of approximately 0.95 cm^2. The Strat-M® membrane was placed in between the donor and the receptor compartment and secured tightly using a horseshoe clamp. The optimized formulations of TRF ethosomes (TRF30 and TRF40) and the control (40% ethanolic TRF solution) were loaded in the donor compartments. Whereas, the receptor compartment was filled with phosphate buffered saline (PBS) containing polysorbate 80 (1% w/v). The diffusion cells were placed on a magnetic stirring block where the receptor compartment was submerged in a water bath maintained at 37 ºC. Samples were withdrawn (200 µL) from the receptor compartment at predetermined time points up to 48 hours and analysed by HPLC, n=4. Permeation profile curves were generated by plotting the cumulative amount of drug permeated (µg/cm^2) against time (hr). The steady state flux (*J*) which represents the amount of tocotrienol permeated per unit area was determined from the gradient of the linear portion of the plot (Nair R. S. and Nair 2015).

***Ex vivo* skin permeation studies using full-thickness human skin and heat separated epidermal membrane.**

Skin samples were obtained post-abdominoplasty from a local clinic in Kuala Lumpur, Malaysia after obtaining the Ethics approval from the Science and Engineering Research Ethics Committee (SEREC), University of Nottingham Malaysia (Ethics approval No: RS010516). A participant information sheet had been given to subjects with clear information about the type of research being carried out and about the disposal of their donated skin. Skin samples were collected after obtaining consent from patients and the excised skin samples were brought to the lab immediately after surgery. The subcutaneous fat was removed by blunt dissection and the skin was subsequently cut into pieces of approximately 3 cm^2. The processed skin samples

were subsequently wrapped in aluminium foil, sealed in a polythene bag and stored at −20 °C until future use.

The skin permeation experiments were conducted in a similar way as explained for Strat-M® membrane. The diffusion cells were assembled with skin samples where the stratum corneum (SC) layer facing upward and clamped firmly between the donor and the receptor compartments, n=5. TRF ethosome (equivalent to 1 mg gamma-T3) was taken in the donor phase whereas, the receptor phase contained PBS pH 7.4 with 1% polysorbate 80 and sodium azide (0.02% w/v). Sodium azide was used as an antibacterial agent to prevent microbial growth that likely to arise from the skin on prolonged exposure at 37 °C. The receptor samples were withdrawn at regular intervals and analysed by injecting 10 µL samples to an UHPLC system (Waters, Acquity® Arc™) equipped with a fluorescence detector (2475 FLR). A reverse phase column (CORTECS® C18, 2.7 µm, 50 mm length × 4.6 mm diameter), maintained at 25 ± 5 °C was employed for gamma-T3 quantification. The mobile phase consisted of a mixture of methanol and water (95:05) with a flow rate maintained at 1.0 mL/minute. The detector excitation and emission wavelengths were 295 nm and 330 nm respectively. Permeation studies were was also carried out using the heat separated epidermal membrane. The full-thickness human skin was immersed into de-ionised water (60 °C) for 1 minute and the epidermal layer was carefully peeled away using forceps. Experiments were conducted similar to that with full-thickness skin with the only exception being that epidermal membrane was used instead of full-thickness skin, n=5.

Drug stability studies in skin extract and the receptor media

Stability of the permeant on exposure to the receptor media and the skin extract were assessed. Firstly, full-thickness human skin weighing 10 g was minced on white ceramic tile using a scalpel blade and placed in a glass bottle containing 50 mL of PBS pH 7.4 with 1% polysorbate 80. The mixture was then placed on a shaker incubator at 37 °C and macerated for 24 hours at

200 rpm. The skin extract was filtered through a Whatman® filter paper (110 nm diameter and 11 µm pore size), and 2 mL of the extract was added to a specified quantity (100 µg) of drug solution in a glass sample bottle. These drug solutions were then incubated in a water bath at 37 °C for 72 hours and at pre-determined time intervals (0, 6, 12, 24, 48, 72 hours), samples were removed and analysed by using the HPLC method. In a similar manner, permeant stability in the receptor media without the skin extract (PBS pH 7.4 + 1% polysorbate 80) was also assessed to provide a clearer picture around potential degradation issues during the permeation studies using Strat-M® membrane.

***In vitro* cytotoxicity study on HaCat cells**

Cytotoxicity of the pure TRF and the formulations was evaluated using MTT assay as reported previously (Nair Rajesh Sreedharan et al. 2019). The HaCat cells (human keratinocyte cells) were grown in DMEM media with 10% fetal bovine serum and 1% penicillin-streptomycin. The fully confluent cells were seeded in a 96-well plate (5×10^3 cells/well) and incubated at 37 °C maintaining 5% CO_2 for about 24 hours leaving the cells to adhere onto the 96-well plate. Thereafter, the media was removed, and the cells were treated with the formulations and the pure drug solutions. The untreated cells maintained at the same experimental conditions were used as the control. The plates were incubated for 72 hours and 20 µL MTT solution (5mg/mL in sterile PBS) was added to each well and further incubated for 4 hours. The purple coloured formazan crystals formed was then solubilised by adding DMSO (100 µL) and the absorbance was measured at 570 nm using a microplate reader (Biotek Instruments, Inc USA), n=3. The percentage cell viability was calculated on 48 and 72-hour incubation (Nair Rajesh Sreedharan et al. 2019; Scolari et al. 2019).

Statistical analysis

Statistical analysis was done using Graph-Pad Prism software version 7.03. All values are expressed as a mean ± standard deviation. The statistical significance between two groups was

done using Student's *t*-test, more than two sets of data was tested by one-way analysis of variance (ANOVA) followed by post-hoc Tukey-HSD (Honestly Significant Difference), $p < 0.05$ was considered significant.

Results and Discussion

Formulation of TRF loaded ethosomes

Ethosomes were successfully developed by the film evaporation technique (Touitou et al. 2000). Optimisation was performed by varying the phospholipid concentration, ethanol content, sonication time and the sonication amplitude. Reports suggest that a particle size < 300 nm is suitable for passive transport across the skin (Verma DD et al. 2003; Verma Poonam and Pathak 2012). Therefore, we aimed to restrict the ethosome sizes to below 300 nm by modulating the formulation variables. TRF ethosomes ethosomes were in the size range of 64.9 ± 2.2 (TRF-40) to 79.6 ±3.9 nm (TRF-30), where the ZP was found to be -53.3 ± 2.5 and -62.0 ± 2.6 mV correspond to TRF-40 and TRF-30 respectively. It was observed that when the ethanol concentration was increased from 30% to 40% the vesicle size decreased (Figure 1a). However, further increasing the ethanol concentration up to 50% led to the production of large vesicles (219.4 ± 6.3 nm). Ethanol concentration above a certain level may soften the lipid bilayer within the ethosome, compromising on the structural integrity and encapsulation efficiency (Fang et al. 2008; Ahad et al. 2013). Therefore, TRF-30 and TRF-40 were selected for further analysis.

Vesicle size showed a direct relationship with increasing phosphatidylcholine concentration in the formulation; this is in line with previous reports (Pathan et al. 2018). Here, the phospholipid concentration was varied between 0.5 % w/v and 2.0 %w/v. The vesicle size of ethosomes prepared using 0.5 % phospholipid was greater than those prepared with 1.0 % w/v phospholipid; this was possibly due to the vesicles being imperfectly formed. This was evident from the higher PDI value obtained at a concentration of 0.5 % (0.78) as compared to

1% (0.24). The SPC concentration was optimised as 1.0 % w/v with the vesicle size from this formulation being smallest with a low PDI (Figure 1 b). A uniform size distribution was observed with an SPC concentration of 1.0% w/w giving PDI values < 0.25. Furthermore, the ZP has a significant influence on the stability of vesicles: a high positive or negative ZP results in greater repulsion between vesicles as this is indicative of a more disperse electrical double-layer which increases the likelihood of repulsion between adjacent particles and therefore reduces chance of aggregation. Studies have shown that ZP values higher than +/−30 mV exhibit significant electrostatic repulsion between the adjacent particles and can prevent the fusion of vesicles (Freitas and Müller 1998).

The effect of sonication amplitude on ethosome formation was evaluated at amplitudes of 20%, 30% and 40%, and the effect of sonication duration was also tested by measuring the ethosome size at different time intervals (0, 10, 30 and 60 seconds). The results showed that vesicle size was inversely related to the sonication time and the amplitude (Figure 1 c & d). At low sonication amplitudes (20% and 30%) there was no significant difference seen in the average vesicle size however, 40% amplitude caused a significant reduction in the mean vesicle size. Higher sonication amplitudes and longer durations of sonication can possibly disrupt the ethosome structure. Silva et al. also reported that vesicle size was reduced on increasing the sonication amplitudes (Silva et al. 2010) and it has also been reported that high amplitudes (>40%) may generate heat and if the temperature exceeds 50°C then it may cause the hydrolysis of phosphatidylcholine. For these reasons, an amplitude of 20% for 60 s was employed throughout the study.

STEM analysis

Ethosomes imaging was performed by STEM. This technique combines the principle of SEM and TEM and was performed using the FE-SEM machine with an additional imaging holder to support a copper grid. The images of the optimised ethosomes showed a spherical shape with

smooth edges (Figure 2). No fusion or aggregation was observed indicating a homogeneous distribution of ethosomes, this was in agreement with the low PDI (< 0.25) obtained from Zetasizer analysis. However, the vesicle size data were slightly greater than those obtained with Zetasizer. The DLS measurements provide the average hydrodynamic diameter of a relatively high volume of colloidal suspension whereas the STEM images illustrate individual particles, i.e. a very low sample volume. Therefore, a combination of DLS measurements with imaging techniques can provide a better interpretation (Eaton et al. 2017).

Encapsulation efficiency

The encapsulation efficiencies of the TRF ethosomes were 66.8 ± 1.9% and 68.5 ± 1.2% correspond to TRF-30 and TRF-40 respectively, and no significant differences (p >0.05) found between TRF-30 and TRF-40. Reports suggest that ethanol can increase the EE of both hydrophilic and lipophilic drugs. Ethanol is effectively acting as a co-solvent enabling a larger amount of drug to be entrapped in the lipid bilayer (Dubey et al. 2007). High EE with an optimum vesicle size helps to maximise the transdermal delivery of drugs via vesicular carriers.

FTIR analysis

FTIR analyses of TRF and the formulation additives were performed to determine whether any structural changes had occurred during the formulation process (Figure 3). Prominent peaks from TRF were recorded at the following wavenumbers: 3423.4 cm^{-1} O−H stretching vibration, 2923.7 cm^{-1} and 2853.85 cm^{-1} CH_2 stretching, 1723.01 cm^{-1} C=C stretch, 1453 cm^{-1} C-H bend and 1377.04 cm^{-1} −C−C− stretch. SPC showed distinctive peaks at: 2923.0 cm^{-1} probably due to CH_2 stretching vibration, 1736.6 cm^{-1} saturated aliphatic carbonyl (C=O) stretching vibration, 1614.8 cm^{-1} N−H bend of primary amines, and 1460.7 cm^{-1} C−H bending of CH_3. A characteristic phosphate (PO_4) stretch was seen at 1052.9 cm^{-1} and the quarternary amino stretching at 1227 cm^{-1} (Nzai and Proctor 1998). In the spectrum for cholesterol, a weak band at 3394.4 cm^{-1} corresponds to the O−H stretching vibration, peaks at 2930.5 cm^{-1} and 2856.3

cm^{-1} are due to CH_2 stretching vibration, the bands at 1462.5 cm^{-1} and 1364.9 cm^{-1} are −C−C− aromatic stretching and C−O stretching respectively. It is evident from the individual spectra that many common functional groups were present in the excipients and the active drugs. This could potentially lead to the shifting of peaks to lower or higher wave numbers in the final formulation. However, the characteristics peaks described above for TRF were visible in the respective ethosome spectra suggesting that TRF was compatible with the formulation additives.

Permeant solubility studies and the design of the receptor phase medium

In an attempt to find a suitable receptor medium, saturation solubilities of TRF (gamma-T3) were determined in various vehicles (Table 2). TRF was found to be practically insoluble in PBS 7.4, and very poorly soluble in PBS containing 40% ethanol. However, TRF demonstrated an enhanced solubility in PBS containing 1% w/v polysorbate 80, a surfactant which has previously been shown to help maintain sink conditions (Ruela et al. 2016). Therefore, PBS containing 1% w/v polysorbate 80 was used as the preferred receptor phase considering its superiority in solubilising the drug and its minimal effect on membrane integrity. *In vitro* permeation studies using Franz-type diffusion cells generally exhibit a steady state drug diffusion profile under perfect sink conditions. It has been suggested that the drug concentration in the receptor phase should be much lower than the saturation solubility to ensure that permeant dissolution is not a rate-limiting step (Singh et al. 2018). The maximum receptor concentration obtained after 48h permeation study was less than 2% of the saturation solubility of TRF, thus ensuring a perfect sink condition.

***In vitro* permeation of TRF from ethosomal formulations across Strat-M® membrane**

The permeation of TRF from the ethosomal formulations was shown to be significantly higher than from the control (40% ethanolic TRF) (Figure 4). Furthermore, there was also found to be

a significant difference in the cumulative amount permeated after 48 hours between the two ethosomal formulations, i.e. TRF30 and TRF40 ($p < 0.05$). TRF40 showed a greater cumulative amount permeated after 48 hours (132.38 ± 10.84 µg cm^{-2}) and a higher flux (3.15 ± 0.28 µg cm^{-2} h^{-1}). Whereas, TRF30 showed a cumulative permeation and flux of 87.44 ± 7.72 µg cm^{-2} and 2.07 ± 0.20 µg cm^{-2} h^{-1} respectively. These significant differences in amount permeated and flux could be due to the differences in ethanol content. Studies have shown that gamma-T3 permeation from TRF nanoemulsions across a cellulose-ester membrane (CM) gave a flux of 0.39 µg cm^{-2} hr^{-1} (Pham et al. 2016), which was much lower than the flux obtained using ethosomal formulations (TRF30 or TRF40) in our study. CM is employed in many permeation studies but they are simple porous membranes with no inherent rate controlling property as such, the flux values will not be directly comparable to those obtained using Strat-M® membranes (Haq et al. 2018). Although the structure of Strat-M® is complex and offers greater resistance to diffusion than CM, the gamma-T3 flux obtained from the ethosomal formulations was at least 5-fold greater than from TRF nanoemulsions reported in Pham et al. study. This clearly shows the advantages of ethosomal formulations in enhancing the permeation of highly lipophilic compounds such as TRF.

***Ex vivo* permeation of TRF from ethosomal formulations across full-thickness human skin**

The skin permeation studies of ethosomal formulation (TRF-40) showed promising results than the control solution. The cumulative amount of gamma-T3 permeated with TRF-40 was 1.03 ± 0.24 µg cm^{-2} with the corresponding flux value being 0.03 ± 0.01 µg cm^{-2} h^{-1} (Figure 5a), and this was much lower compared to the results obtained using Strat-M®. Such a large difference in flux is attributable to the significant differences between the morphology of skin and the artificial membrane. It is to be agreed with the facts that, the SC layer remains to be the main checkpoint in the skin permeation. The corneocytes in the SC are tightly bound and play a key

role in maintaining the barrier properties of the skin (Sapra et al. 2012). Reports suggest that ethosomes can permeate under both occluded and non-occluded conditions (Dayan and Touitou 2000). Therefore, to avoid solvent loss due to evaporation and to keep the donor phase hydrated, occluded conditions were maintained throughout our experiments. There are a number of suggested mechanisms for ethosomal skin permeation. Most studies report a synergistic effect between ethanol and the vesicular components. A high ethanol concentration and the malleable nature of the ethosomes would have favoured transdermal permeation. Touitou et al. explained the skin permeation of ethosomes with regards to the "softening" of SC lipids (Touitou et al. 2000). Ethanol can interact with the polar head groups of the lipid molecules thereby causing a transition of the SC lipids resulting in enhanced fluidity. This can augment membrane permeability, thereby permitting the passage of vesicles through the tiny pores of the skin (Verma P. and Pathak 2010; Pandey et al. 2015). Alternatively, it has been suggested that phospholipids present in ethosomes may interact with SC lipids, possibly altering the transition temperature which may facilitate enhanced permeation (Yang et al. 2017). The surface charge of vesicles also plays a significant role in transdermal permeation. Reports suggest that negatively charged vesicles exhibit enhanced skin permeation as compared to those that are positively charged (Ogiso et al. 2001). It is possibly due to the repulsion between the vesicles and the negatively-charged skin lipids, that may create a transient opening leading to enhanced skin permeation (Kohli and Alpar 2004).

Permeation studies of TRF ethosomes using heat separated epidermal membrane

The flux and the cumulative permeation of TRF-40 after 48 hours was 0.04 ± 0.01 µg cm^{-2} h^{-1} and 1.73 ± 0.29 µg cm^{-2} respectively. This result indicated that the flux of gamma-T3 from the ethosomal formulation across the epidermal membrane was significantly higher than that across full thickness human skin ($p < 0.05$) (Figure 5b). This discrimination observed between the two different biological membranes is largely due to the differences in the physiological

structures and the impact of physicochemical properties, namely the MW and the log *P* of the permeant (Potts and Guy 1992). Gamma-T3 is highly lipophilic with a log *P* of 8.9 and MW 411 Da. Reports have shown that SC stripping causes an enormous increase in permeation, confirming that the SC is the principal barrier to transdermal delivery (Andrews et al. 2013). Fick's first law states that the membrane thickness is inversely proportional to the rate of diffusion. Therefore, with the epidermis being thinner than full-thickness skin, higher permeation was anticipated. The SC and the underlying dermis layer depict the lipophilic and aqueous regions respectively. Ethosomes, being highly deformable, can penetrate the SC and subsequently fuse with skin lipids and thereby release their encapsulated drug into the deeper layers of the skin. The highly lipophilic gamma-T3 (log *P* 8.9) may diffuse slower through the relatively hydrophilic dermis layer. For the reasons outline above it can be concluded that the flexible nature of ethosomes and the lipophilicity of TRF favour passage through the SC and epidermis, whilst diffusion through the relatively hydrophilic dermis layer may cause higher resistance. This could be one of the possible reasons for the enhanced permeation observed through the epidermal layers as compared to full-thickness skin. Our results were in agreement with a previous simulation study, suggesting that highly lipophilic compounds easily pass through SC whereas a slow diffusion was reported through viable epidermis and the dermis layer (Yamaguchi et al. 2008).

Drug stability in skin extract and in the receptor media

Drug stability studies in the receptor phase media were conducted at 37 °C, the receptor phase temperature. Interestingly, reports suggest that polysorbates, of which polysorbate 80, significantly enhance the stability of hydrophobic drugs through the formation of micelles and support the appropriateness of polysorbate 80 in the diffusion medium. TRF showed enhanced stability in the media containing skin extract compared to the media alone (Figure 6). This could be due to the ionic interaction or hydrogen bonding between the drug and the skin

components. Protonated groups present in tocotrienols might have interacted with the negatively charged skin proteins which would have formed strong ionic linkages, and the crosslinks formed between the skin proteins might have enhanced the thermal stability of TRF.

***In vitro* cytotoxicity on healthy HaCat cells**

The skin compatibility of TRF ethosomal formulations was evaluated using healthy HaCat cells. There were significant differences in cell viability when a pure TRF solution and the TRF-loaded ethosomal formulations were tested. A concentration-dependent reduction in cell viability was observed (72 hours) where the % cell viability at the highest drug concentration (50 µg/mL) correspond to TRF solution was found to be 10.9 ± 3.7% and for TRF ethosomes it was 84.9 ± 6.7% (Figure 7). Moreover, the blank ethosomes also showed a high % cell viability (>95%), indicating the apparent skin compatibility of excipients used in the formulation of ethosomes. This suggests that any cytotoxicity demonstrated was due to the drug TRF and not from the carrier system. These results corroborate previous reports which suggested that ethosomal formulations had a low toxicity to normal cells (Marto et al. 2016). Xie et al. reported a similar cytotoxicity of drug-free ethosomes on healthy fibroblast cells (>90% cell viability), further supporting the biocompatibility of ethosomal carriers (Xie et al. 2018). Reports have also revealed that lipid vesicles may have a protective effect on HaCat cells, suggesting that the phospholipid content could be the possible reason for enhanced cell viability as compared to non-vesicular TRF solutions (Liu et al. 2013; Avadhani et al. 2017).

Conclusion

Ethosomes containing TRF were successfully formulated and evaluated *in vitro*. The vesicle size and ZP were optimised for transdermal delivery and colloidal stability. Permeations studies using full-thickness human skin showed that gamma-T3 flux from the ethosomal formulations was significantly higher than that of a TRF solution. Furthermore, the drug flux across the

Strat-M® and the epidermal membrane was found to be higher than that across full-thickness skin ($p < 0.05$). Cytotoxicity studies on healthy HaCat cells supported the notion that TRF ethosomal formulations are safe and possess great potential for transdermal delivery. Further *in vivo* evaluations should be conducted in order to validate these *in vitro* data.

Acknowledgements

The authors would like to acknowledge the Faculty of Science at the University of Nottingham Malaysia (UNM) for the financial support towards this project. We are grateful to ExcelVite Sdn. Bhd. (Perak, Malaysia) for providing TRF and tocotrienol standards.

Conflict of Interest

The authors declare that there are no conflicts of interest

Funding

The present work was funded by the University of Nottingham Malaysia (UNM) and through the open access funding provided by the Qatar National Library.

References

Aggarwal BB, Kumar A, Bharti AC. 2003. Anticancer potential of curcumin: preclinical and clinical studies. Anticancer Research. 23(1/A):363-398.

Ahad A, Aqil M, Kohli K, Sultana Y, Mujeeb M. 2013. Enhanced transdermal delivery of an anti-hypertensive agent via nanoethosomes: statistical optimization, characterization and pharmacokinetic assessment. International Journal of Pharmaceutics. 443(1-2):26-38.

Alqahtani S, Alayoubi A, Nazzal S, Sylvester PW, Kaddoumi A. 2013. Nonlinear absorption kinetics of self-emulsifying drug delivery systems (SEDDS) containing tocotrienols as lipophilic molecules: in vivo and in vitro studies. The AAPS journal. 15(3):684-695.

Alqahtani S, Alayoubi A, Nazzal S, Sylvester PW, Kaddoumi A. 2014. Enhanced solubility and oral bioavailability of γ-tocotrienol using a self-emulsifying drug delivery system (SEDDS). Lipids. 49(8):819-829.

Andrews SN, Jeong E, Prausnitz MR. 2013. Transdermal delivery of molecules is limited by full epidermis, not just stratum corneum. Pharmaceutical Research. 30(4):1099-1109.

Avadhani KS, Manikkath J, Tiwari M, Chandrasekhar M, Godavarthi A, Vidya SM, Hariharapura RC, Kalthur G, Udupa N, Mutalik S. 2017. Skin delivery of epigallocatechin-3-gallate (EGCG) and hyaluronic acid loaded nano-transfersomes for antioxidant and anti-aging effects in UV radiation induced skin damage. Drug Delivery. 24(1):61-74.

Barry BW. 2001. Novel mechanisms and devices to enable successful transdermal drug delivery. European Journal of Pharmaceutical Sciences. 14(2):101-114.

Brownlow B, Nagaraj VJ, Nayel A, Joshi M, Elbayoumi T. 2015. Development and In Vitro Evaluation of Vitamin E-Enriched Nanoemulsion Vehicles Loaded with Genistein for Chemoprevention Against UVB-Induced Skin Damage. Journal of Pharmaceutical Sciences. 104(10):3510-3523.

Dayan N, Touitou E. 2000. Carriers for skin delivery of trihexyphenidyl HCl: ethosomes vs. liposomes. Biomaterials. 21(18):1879-1885.

Dubey V, Mishra D, Dutta T, Nahar M, Saraf D, Jain N. 2007. Dermal and transdermal delivery of an anti-psoriatic agent via ethanolic liposomes. Journal of Controlled Release. 123(2):148-154.

Eaton P, Quaresma P, Soares C, Neves C, de Almeida MP, Pereira E, West P. 2017. A direct comparison of experimental methods to measure dimensions of synthetic nanoparticles. Ultramicroscopy. 182:179-190.

Fang Y-P, Tsai Y-H, Wu P-C, Huang Y-B. 2008. Comparison of 5-aminolevulinic acid-encapsulated liposome versus ethosome for skin delivery for photodynamic therapy. International Journal of Pharmaceutics. 356(1-2):144-152.

Freitas C, Müller RH. 1998. Effect of light and temperature on zeta potential and physical stability in solid lipid nanoparticle (SLN™) dispersions. International Journal of Pharmaceutics. 168(2):221-229.

Haq A, Dorrani M, Goodyear B, Joshi V, Michniak-Kohn B. 2018. Membrane properties for permeability testing: Skin versus synthetic membranes. International Journal of Pharmaceutics. 539(1):58-64.

Hasan ZAA, Idris Z, Gani S, Basri M. 2018. In vitro safety evaluation of palm tocotrienol-rich fraction nanoemulsions for topical application. J Oil Palm Res. 30:150-162.

Heeremans JL, Gerritsen HR, Meusen SP, Mijnheer FW, Gangaram Panday RS, Prevost R, Kluft C, Crommelin DJ. 1995. The preparation of tissue-type Plasminogen Activator (t-PA) containing liposomes: entrapment efficiency and ultracentrifugation damage. Journal of Drug Targeting. 3(4):301-310.

Jose A, Labala S, Ninave KM, Gade SK, Venuganti VVK. 2018. Effective Skin Cancer Treatment by Topical Co-delivery of Curcumin and STAT3 siRNA Using Cationic Liposomes [journal article]. AAPS PharmSciTech. 19(1):166-175.

Kohli AK, Alpar HO. 2004. Potential use of nanoparticles for transcutaneous vaccine delivery: effect of particle size and charge. International Journal of Pharmaceutics. 275(1):13-17.

Ling MT, Luk SU, Al-Ejeh F, Khanna KK. 2012. Tocotrienol as a potential anticancer agent. Carcinogenesis. 33(2):233-239.

Liu D, Hu H, Lin Z, Chen D, Zhu Y, Hou S, Shi X. 2013. Quercetin deformable liposome: Preparation and efficacy against ultraviolet B induced skin damages in vitro and in vivo. Journal of Photochemistry and Photobiology B: Biology. 127:8-17.

Manickam B, Sreedharan R, Chidambaram K. 2019. Drug/Vehicle Impacts and Formulation Centered Stratagems for Enhanced Transdermal Drug Permeation, Controlled Release and Safety: Unparalleled Past and Recent Innovations-An Overview. Current Drug Therapy. 14(3):192-209.

Marto J, Vitor C, Guerreiro A, Severino C, Eleutério C, Ascenso A, Simões S. 2016. Ethosomes for enhanced skin delivery of griseofulvin. Colloids and Surfaces B: Biointerfaces. 146:616-623.

Mba OI, Dumont M-J, Ngadi M. 2015. Palm oil: Processing, characterization and utilization in the food industry – A review. Food Bioscience. 10:26-41.

Nainwal N, Jawla S, Singh R, Saharan VA. 2019. Transdermal applications of ethosomes – a detailed review. Journal of Liposome Research. 29(2):103-113.

Nair RS, Morris A, Billa N, Leong C-O. 2019. An Evaluation of Curcumin-Encapsulated Chitosan Nanoparticles for Transdermal Delivery [journal article]. AAPS PharmSciTech. 20(2):69.

Nair RS, Nair S. 2015. Permeation Studies of Captopril Transdermal Films Through Human Cadaver Skin. Curr Drug Deliv. 12(5):517-523.

Nzai JM, Proctor A. 1998. Determination of phospholipids in vegetable oil by fourier transform infrared spectroscopy [journal article]. Journal of the American Oil Chemists' Society. 75(10):1281-1289.

Ogiso T, Yamaguchi T, Iwaki M, Tanino T, Miyake Y. 2001. Effect of positively and negatively charged liposomes on skin permeation of drugs. Journal of drug targeting. 9(1):49-59.

Pandey V, Golhani D, Shukla R. 2015. Ethosomes: versatile vesicular carriers for efficient transdermal delivery of therapeutic agents. Drug Delivery. 22(8):988-1002.

Pathan IB, Jaware BP, Shelke S, Ambekar W. 2018. Curcumin loaded ethosomes for transdermal application: Formulation, optimization, *in-vitro* and *in-vivo* study. Journal of Drug Delivery Science and Technology. 44:49-57.

Pham J, Nayel A, Hoang C, Elbayoumi T. 2016. Enhanced effectiveness of tocotrienol-based nano-emulsified system for topical delivery against skin carcinomas. Drug Delivery. 23(5):1514-1524.

Potts RO, Guy RH. 1992. Predicting Skin Permeability. Pharmaceutical Research. 9(5):663-669.

Ruela ALM, Perissinato AG, Lino MEdS, Mudrik PS, Pereira GR. 2016. Evaluation of skin absorption of drugs from topical and transdermal formulations. Brazilian Journal of Pharmaceutical Sciences. 52(3):527-544.

Sapra B, Jindal M, Tiwary AK. 2012. Tight junctions in skin: new perspectives. Therapeutic Delivery. 3(11):1297-1327.

Scolari IR, Páez PL, Sánchez-Borzone ME, Granero GE. 2019. Promising Chitosan-Coated Alginate-Tween 80 Nanoparticles as Rifampicin Coadministered Ascorbic Acid Delivery Carrier Against Mycobacterium tuberculosis [journal article]. AAPS PharmSciTech. 20(2):67.

Silva R, Ferreira H, Little C, Cavaco-Paulo A. 2010. Effect of ultrasound parameters for unilamellar liposome preparation. Ultrasonics Sonochemistry. 17(3):628-632.

Singh I, Nair RS, Gan S, Cheong V, Morris A. 2018. An evaluation of crude palm oil (CPO) and tocotrienol rich fraction (TRF) of palm oil as percutaneous permeation enhancers using full-thickness human skin. Pharmaceutical development and technology. 24(4):448-454.

Touitou E, Dayan N, Bergelson L, Godin B, Eliaz M. 2000. Ethosomes — novel vesicular carriers for enhanced delivery: characterization and skin penetration properties. Journal of Controlled Release. 65(3):403-418.

Verma DD, Verma S, Blume G, Fahr A. 2003. Particle size of liposomes influences dermal delivery of substances into skin. International Journal of Pharmaceutics. 258(1-2):141-151.

Verma P, Pathak K. 2010. Therapeutic and cosmeceutical potential of ethosomes: An overview. Journal of Advanced Pharmaceutical Technology & Research. 1(3):274-282.

Verma P, Pathak K. 2012. Nanosized ethanolic vesicles loaded with econazole nitrate for the treatment of deep fungal infections through topical gel formulation. Nanomedicine: Nanotechnology, Biology and Medicine. 8(4):489-496.

Williams AC, Barry BW. 2004. Penetration enhancers. Advanced drug delivery reviews. 56(5):603-618.
Xie J, Ji Y, Xue W, Ma D, Hu Y. 2018. Hyaluronic acid-containing ethosomes as a potential carrier for transdermal drug delivery. Colloids and Surfaces B: Biointerfaces. 172:323-329.

Yamaguchi K, Mitsui T, Aso Y, Sugibayashi K. 2008. Structure–permeability relationship analysis of the permeation barrier properties of the stratum corneum and viable epidermis/dermis of rat skin. Journal of Pharmaceutical Sciences. 97(10):4391-4403.

Yang L, Wu L, Wu D, Shi D, Wang T, Zhu X. 2017. Mechanism of transdermal permeation promotion of lipophilic drugs by ethosomes. International Journal of Nanomedicine. 12:3357-3364.
Yu X, Du L, Li Y, Fu G, Jin Y. 2015. Improved anti-melanoma effect of a transdermal mitoxantrone ethosome gel. Biomedicine & Pharmacotherapy. 73:6-11.
Zhai Y, Xu R, Wang Y, Liu J, Wang Z, Zhai G. 2015. Ethosomes for skin delivery of ropivacaine: preparation, characterization and ex vivo penetration properties. Journal of Liposome Research. 25(4):316-324.

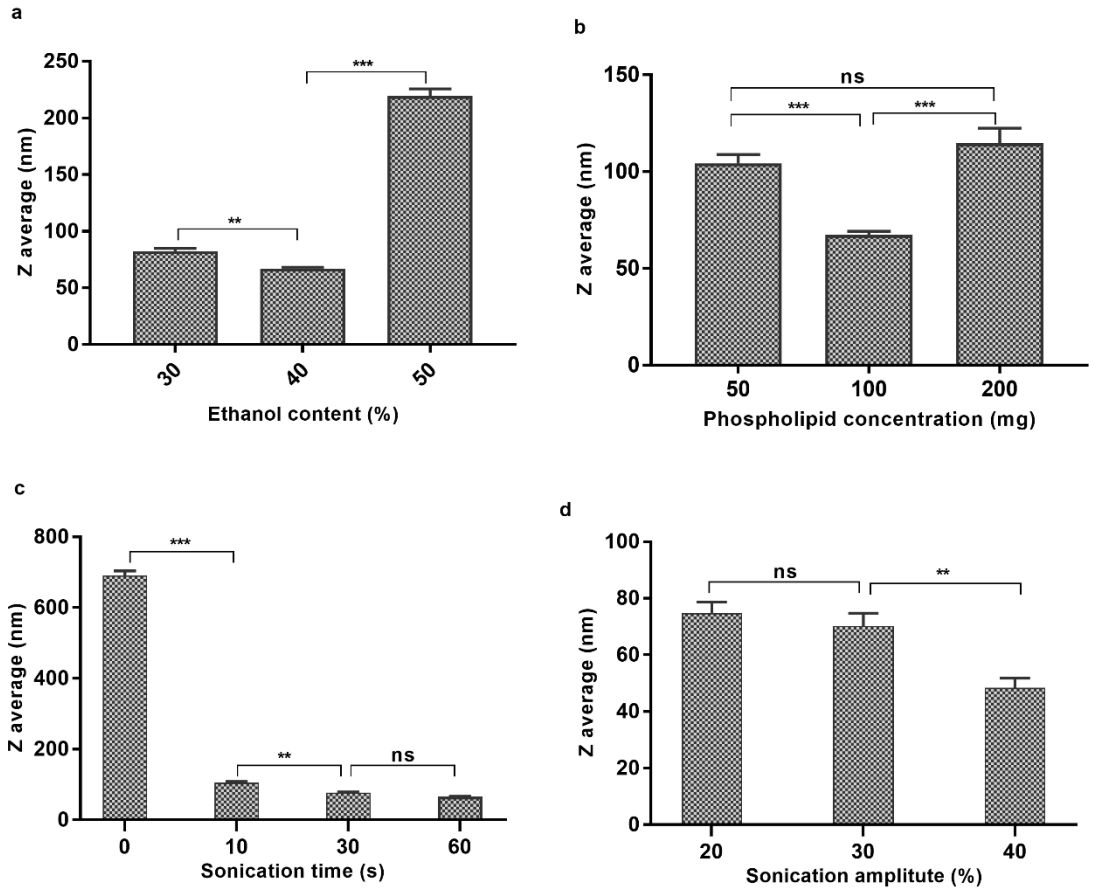

Figure 1. Effect of formulation variables on the ethosome size: (a) Effect of Phospholipid concentration; (b) Effect of ethanol content; (c) Effect of sonication duration and d) Effect of sonication amplitude. Mean ± SD, N=3. (ns: not significant $p > 0.05$; ** $p < 0.002$; *** $p < 0.001$)

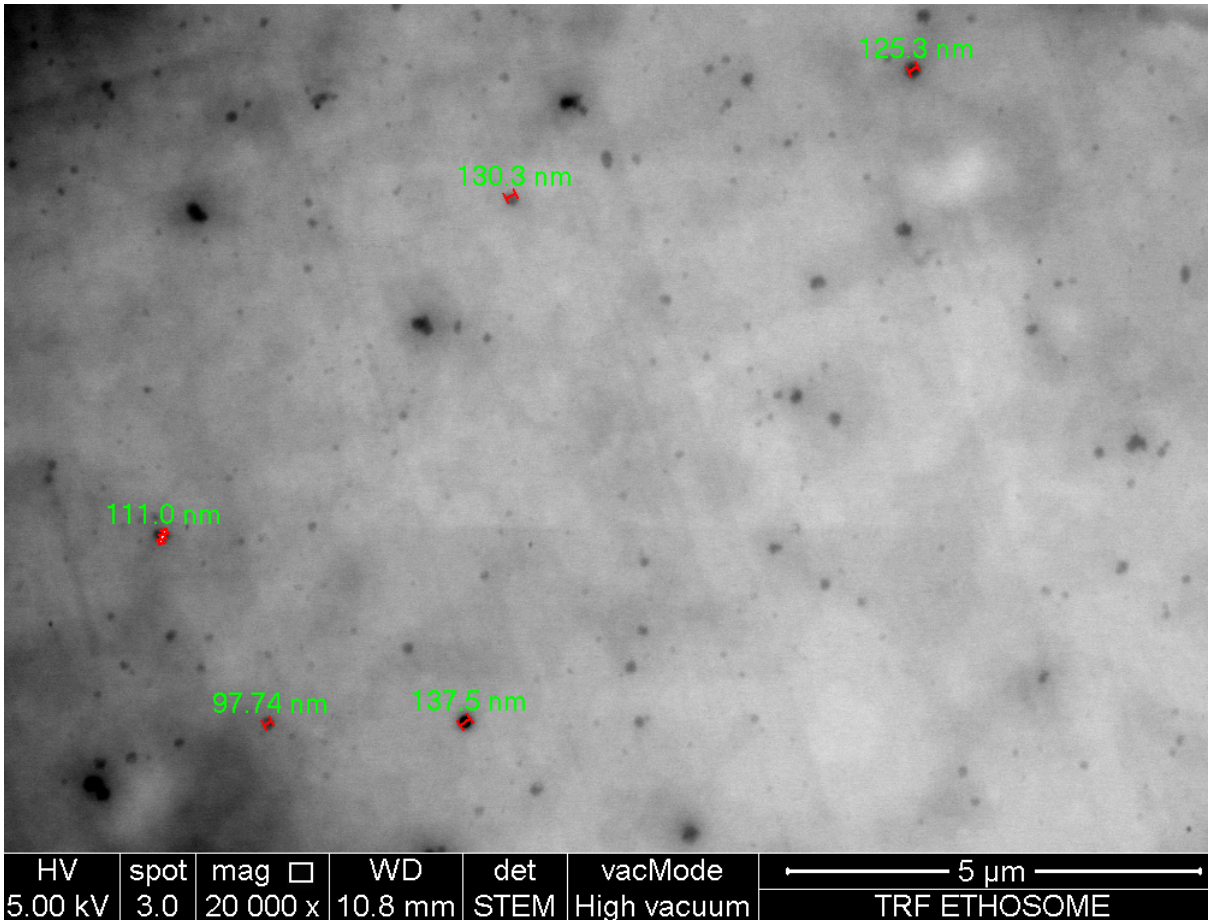

Figure 2. Shows the STEM image of TRF ethosomes.

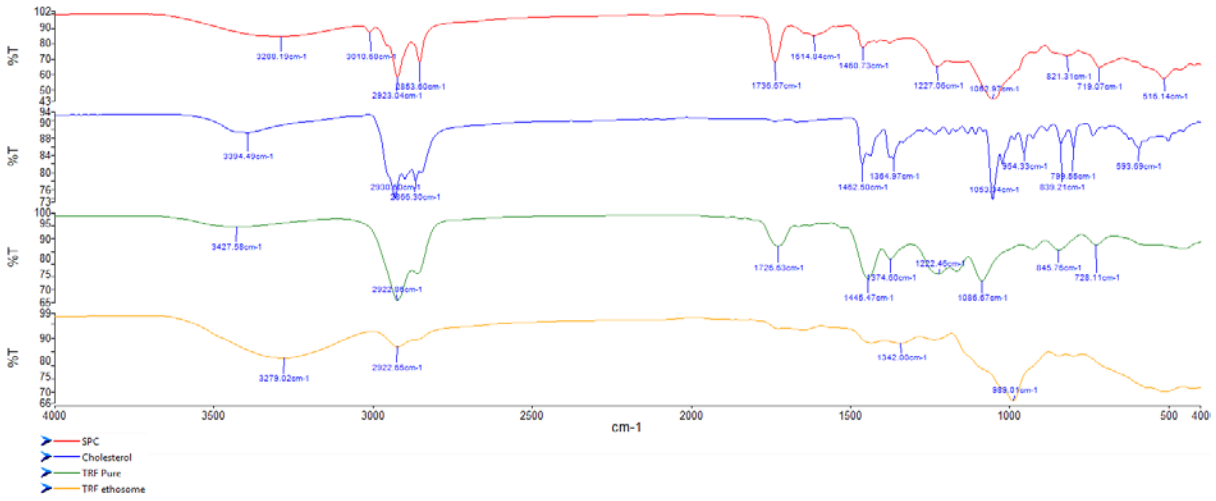

Figure 3. FTIR spectra of SPC, cholesterol, pure TRF and TRF ethosomes.

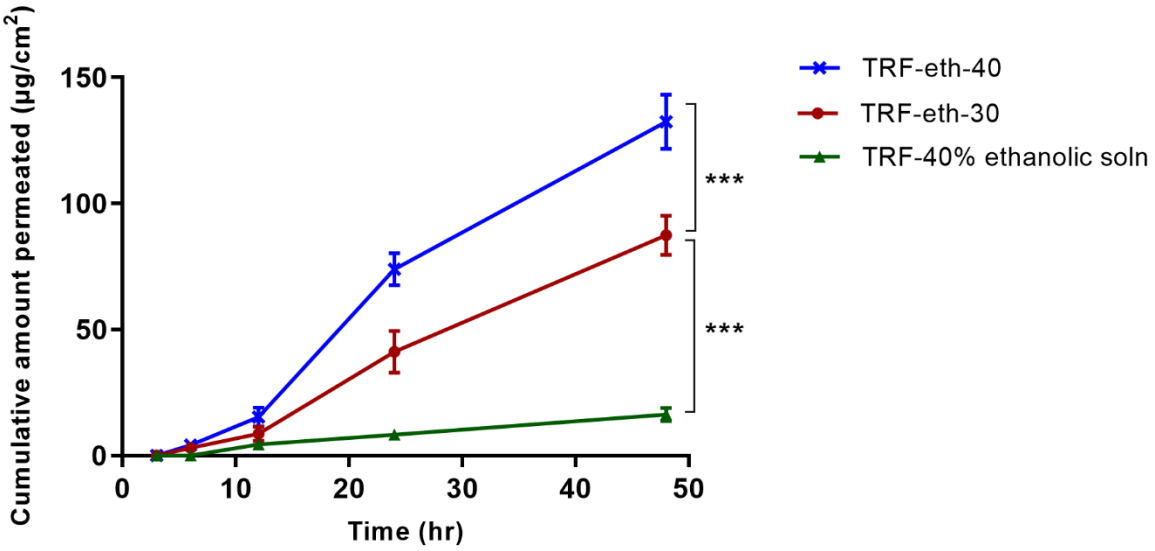

Figure 4. Permeation of gamma-T3 from TRF ethosomes (TRF-30 and TRF-40) and control (TRF in 40% ethanolic solution) through Strat-M® membrane. Mean ± SD, n=4. (*** $p <$ 0.001)

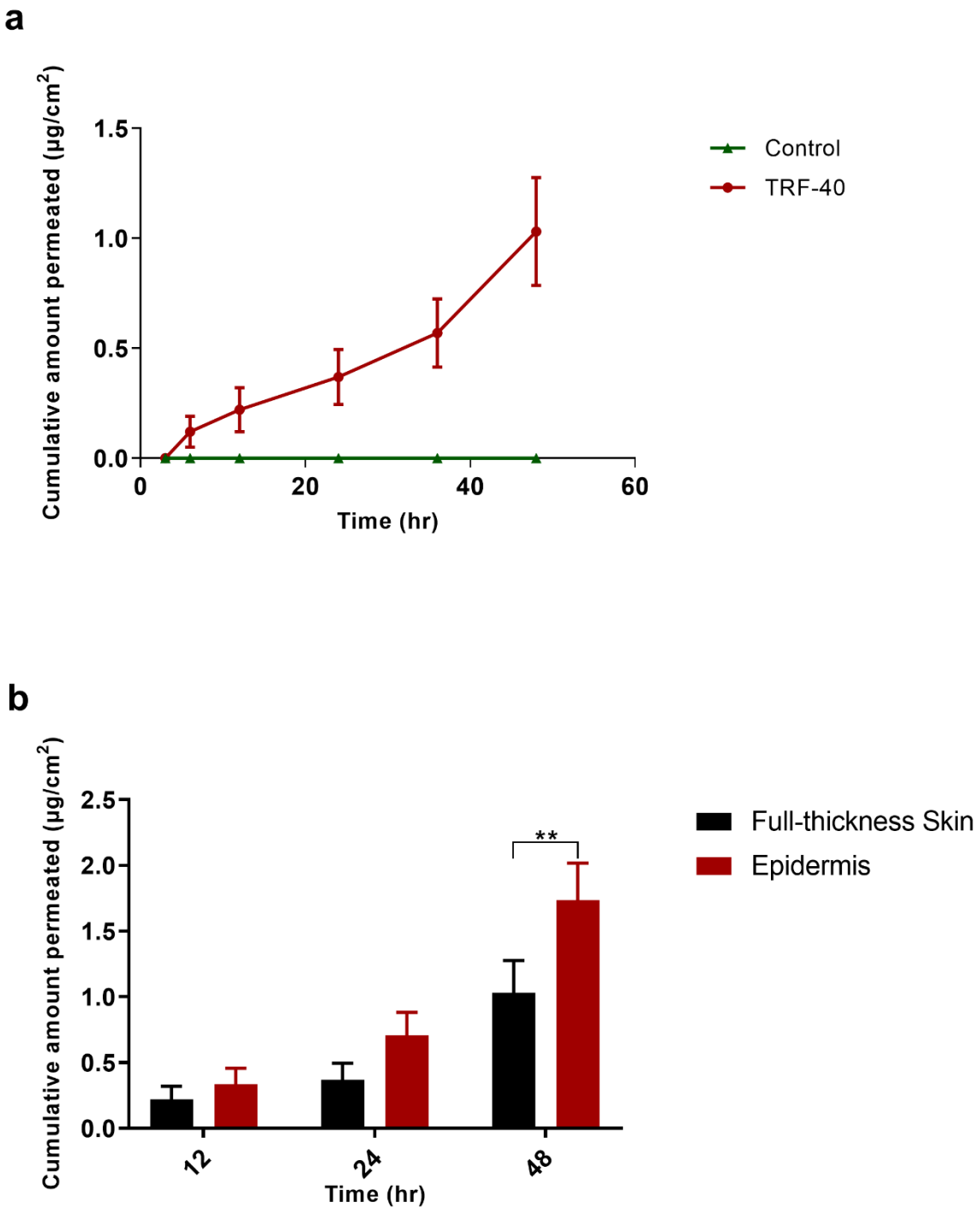

Figure 5. Permeation of gamma-T3 from TRF ethosomes (TRF-40) and control (TRF in 40% ethanolic solution) through excised full-thickness human skin (5a), and a comparison of cumulative gamma-T3 permeated from TRF-40 across the full-thickness human skin and the heat-separated epidermal membrane (5b). Mean ± SD, n=5 (*** $p < 0.001$, ** $p < 0.002$).

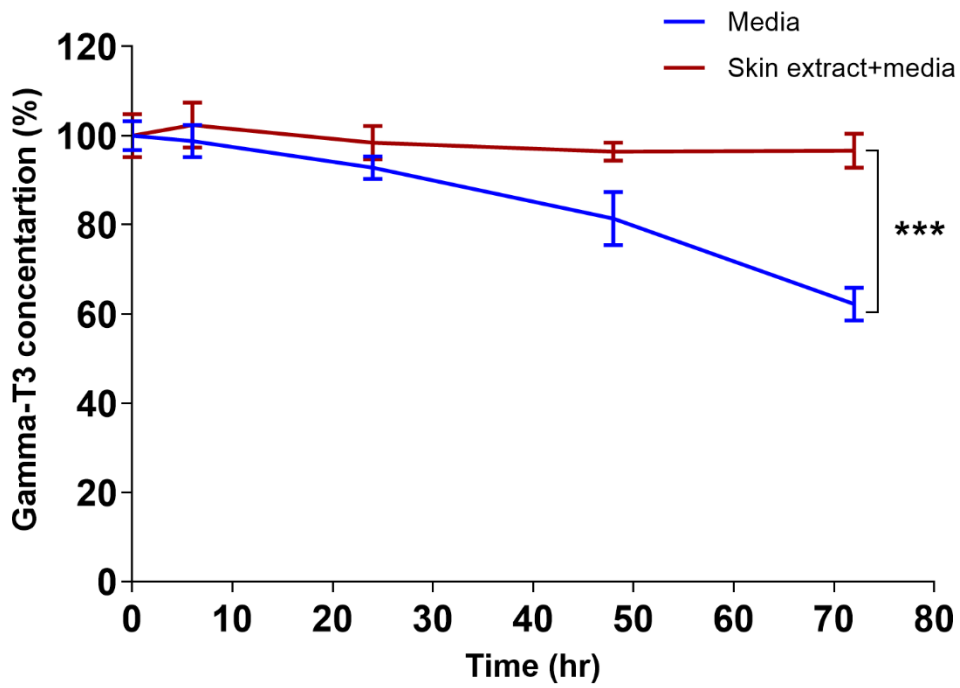

Figure 6. Stability of gamma-T3 in the receptor media at 37 °C showing enhanced stability in the media containing skin extract. Mean ± SD, n=3. (*** $p < 0.001$)

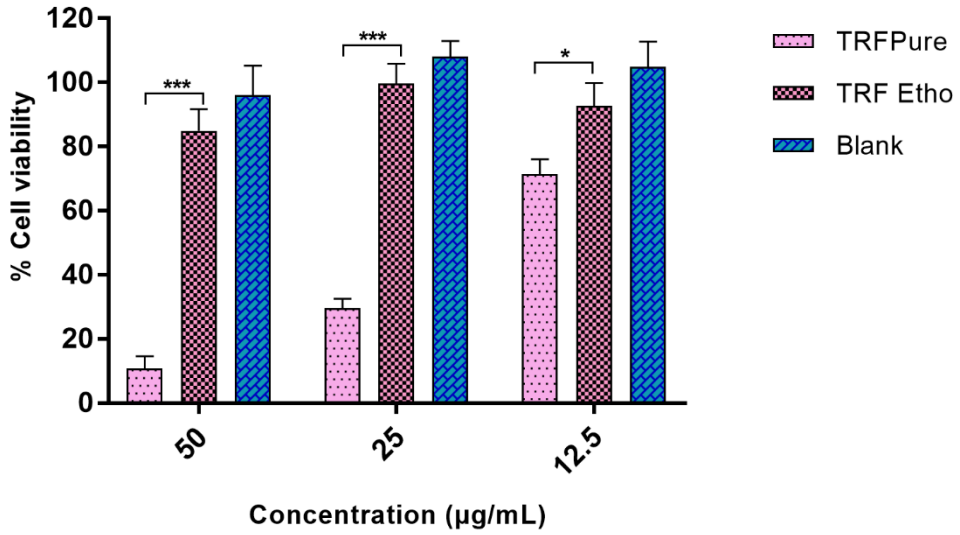

Figure 7. Cell viability of HaCat cells on treatment with TRF solution, blank ethosomes and the TRF ethosomes at three different concentrations (12.5 µg/ml, 25 µg/ml, 50 µg/ml), showing enhanced cell viability of TRF ethosomes than TRF solution. Mean ± SD, *N*=3. (***$p < 0.001$, *$p < 0.033$).

TRF and Palm fruit

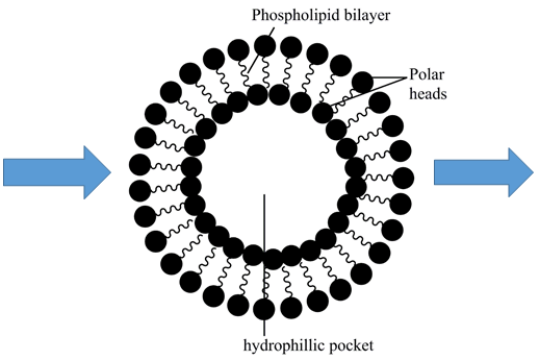

TRF ethosome

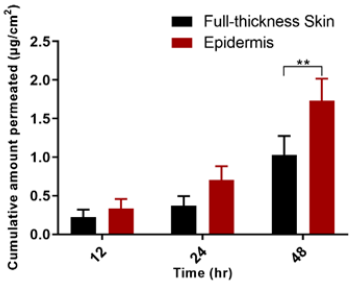

Permeation of TRF ethosome through full-thickness human skin and epidermal membrane

Graphical abstract

Table 1. The composition of the blank and the drug-loaded ethosomal formulations

Ethosome Formulation	Drug (mg)	Phospholipid (mg)	Cholesterol (mg)	Polysorbate 80 (mg)	Ethanol (%)
Blank	-	50	10	10	30
	-	100	10	10	30
	-	200	10	10	30
	-	50	10	10	40
	-	100	10	10	40
	-	200	10	10	40
	-	50	10	10	50
	-	100	10	10	50
	-	200	10	10	50
TRF	10	100	10	10	30
	10	100	10	10	40
	10	100	10	10	50

Table 2. Saturation solubility values of TRF in various vehicles.

Vehicle	Saturation solubility (µg/mL), n=3
PBS	Not detectable
PBS+40% ethanol	16.0 ± 2.0
PBS+1%w/v polysorbate 80	3950.0 ± 47.0